Soft Matter

Accepted Manuscript

ROYAL SOCIETY OF CHEMISTRY

www.rsc.org/softmatter

TOC

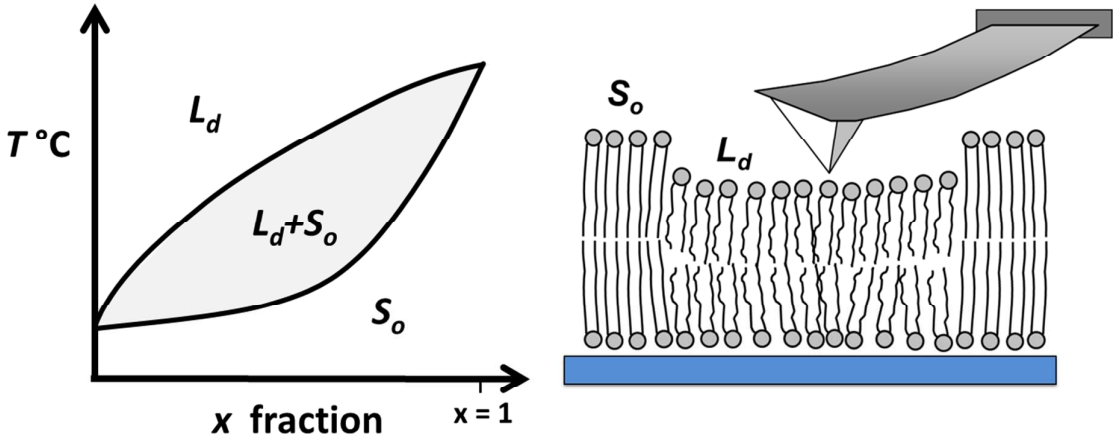

We review the studies dealing with lipid bilayer phase transitions and separations performed by Atomic Force Microscopy highlighting the added values with respect to traditional approaches.

Phase transitions in Supported Lipid Bilayers studied by AFM

Andrea Alessandrini[1,2], Paolo Facci[3]

[1] Dipartimento di Scienze Fisiche, Matematiche e Informatiche, Via Campi 213/A, 41125, Modena

[2] CNR – Istituto Nanoscienze, S3, Via Campi 213/A 41125, Modena, Italy

[3] CNR – Istituto di Biofisica, Via dei Marini 6, 16149, Genova, Italy

Abstract

We review the capabilities of Atomic Force Microscopy (AFM) in the study of phase transitions in Supported Lipid Bilayers (SLBs). AFM represents a powerful technique to cover the resolution range not available to fluorescence imaging techniques and where spectroscopic data suggest that the relevant lateral scale for domain formation might be. Phase transitions of lipids bilayers involve the formation of domains characterized by different height with respect to the surrounding phase and are therefore easily identified by AFM in liquid solution once the bilayer is confined to a flat surface. Even if not endowed with high time resolution, AFM has allows shedding light on some aspects related to lipid phase transitions both in the case of a single lipid component and lipid mixtures containing also sterols. We discuss here the obtained results in light of the peculiarities of Supported Lipid Bilayer model systems.

1 Introduction

For every living cell, the biological membrane represents the site where any exchange between the inside region and the outside world has to transit. These exchanges involve materials, energy and information. A living cell cannot be represented as an equilibrium system, and the biological membrane too is a strongly dynamic system, not at equilibrium, that constantly modifies its structure in order to accomplish different functions. According to these dynamic and out-of-equilibrium characteristics, together with the enormous number of different components that are involved in its formation, the biological membrane exemplifies one of the many biological systems that require tremendous efforts in order to be elucidated from a physical point of view[1]. There is no doubt that understanding biological membranes takes a remarkable advantage from studies on model systems, which are simplified, prototypical representations of a biological membrane that can, in some cases, be considered in equilibrium conditions. Examples of model systems are liposomes, Black Lipid Membranes (BLM) and Supported Lipid Bilayers (SLBs). The mentioned simplification can operate at various levels; from the lowest one, in which a lipid bilayer in the form of a liposome made of a single type of lipid is considered, to systems of increasing complexity that include the presence of different type of lipids (all the way down to the cases in which a lipid composition very similar to that of a cell membrane is considered – Giant Plasma Membrane Vesicles (GPMVs)[2]) and their interaction with models for the cortical actin network[3,4]. Model systems can be exploited both to validate experimental techniques which are going to be used on living cells and to understand the basic and common physical aspect underlying the behavior of biological membranes. Moreover, the observation of a different behavior of model systems with respect to biological membranes can be the starting point for a deeper understanding of the latter. An illustrative case is that represented by the structure of the lipid rafts, for which initial model systems revealed a behavior not found in living cells[5,6]. The observed difference prompted a series of studies, as will be deeply illustrated in this work, which allowed a better definition of the conditions favoring the appearance of lipid rafts in living cells. In particular, the performed studies considered model system of increasing complexity for which the biological behavior was recovered.

Thermodynamics appears ideally suited to tackle problems related to the elucidation of the structure of biological membranes (and of corresponding model systems)[7]. At the heart of many aspects related to membrane structure and associated functions we can consider the possibility of phase transitions and separations according to variation of several parameters. Currently, an increasing number of reports are stressing the possible relevance that a particular thermodynamic state could have on membrane behavior[8]. In particular, the proximity of a membrane to a critical point or a region of critical points could allow explain some aspects of membrane organization, such as dynamic and spatial organization properties. However, the study of these particular thermodynamic conditions, both on model systems and biological membranes of living cells poses great experimental challenges. In fact, to fully accomplish the requirements posed by the investigation of systems near to a critical behavior, the experimental techniques to be used should be endowed with high lateral and time resolution[9]. Single molecule techniques exploiting optical properties of specifically designed probes could provide the required time resolution, but lack

imaging possibilities[10]. Fluorescence microscopy techniques[11] are typically limited in imaging resolution to a scale in the order of some hundreds of nanometers, which seems to be not fully adequate. Spectroscopic techniques such as NMR allow investigating the dynamic properties on the nanometer scale by they require complex interpretations which have to be developed in the specific context of lipid bilayers[12].

Among the techniques able to study the thermodynamic behavior of lipid bilayer model systems[13-15], Atomic Force Microscopy (AFM) emerged as a very powerful tool, mainly due to its remarkable lateral and vertical resolution[16-21]. Exploiting AFM, lipid bilayers can be studied usually in the form of supported bilayers, which means planar lipid bilayers supported by a solid substrate[22,23]. The possibility of controlling environmental chemical composition along with imaging temperature allows AFM to study the thermodynamic behavior of a bilayer as a result of a perturbation. This possibility is connected to the high vertical resolution of the technique and the thickness variations of the lipid bilayer accompanying phase transitions and separations. Moreover, along with imaging capabilities, the AFM provides also force spectroscopy ability (AFS – Atomic Force Spectroscopy)[16]. This last technique allows associate to each phase of the lipid bilayer mechanical information on the nanometer scale that could be relevant to the overall behavior of the membrane. At the same time, a correlation between thermodynamics and mechanics can be established on the basis of this technique. Figure 1 highlights the limits and the useful information that can be retrieved by the different techniques exploited in the field of membrane biophysics.

In this review, we will present the main results obtained with AFM on the investigation of phase transitions of supported lipid bilayers. We will include cases in which both the main phase transition and the phase transition related to lipid-rafts concept are involved.

At the beginning we will briefly introduce the concept of phase transitions in lipid bilayers from a general point of view, considering unsupported systems. We will then present the chemical and physical properties of supported lipid bilayer systems. We will consider some aspects related to the different preparation procedures and how these could impact on the bilayer phase behavior. Afterwards, we will report the main results obtained with AFM in the study of the phase transition of supported lipid bilayers considering phospholipids as bilayer components, comparing the observed features with those available from different techniques that can access thermodynamic properties. We will then include studies of the thermodynamic properties of bilayers that include sterols, a case relevant to the lipid raft concept, and other exogenous molecules. In particular, we will consider the situation of liquid immiscible phases in the supported lipid bilayer. We will also discuss the capabilities of AFM to follow the kinetics of domain nucleation and growth after a temperature jump. A section will be dedicated also to AFS investigations of the mechanical properties of different lipid bilayer phases. In this context we will mainly consider the mechanical resistance of a lipid bilayer to the penetration of an AFM tip. We will exploit this information to draw an ideal bridge connecting bilayer local mechanical properties and gating of ion channels thereby embedded. Lastly, we will discuss possible future developments in terms of relevant pending problems and instrumentation to be developed.

2. A brief introduction to lipid bilayer phase transitions

In this section we will briefly describe the possible phase transitions of lipid bilayers. We will concentrate on thermotropic phase transitions. The lipid bilayer structure is strictly related to the presence of water[24] and, accordingly, phase transitions could also be induced by varying the water fraction with respect to lipids. These sorts of phase transitions are said lyotropic, a common topic for liquid crystal systems, but they we will not be considered in the present work.

Starting from the experimental observation that at low temperature X-ray wide angle diffractions of lipids with fully saturated hydrocarbon chains present very sharp rings which get larger and more diffuse at higher temperatures, it was established that the lipid bilayer phase transition mainly consists in a disordering of the hydrocarbon chains of the lipids[25]. This transition, usually referred to as the main phase transition, consists in a disordering of the hydrophobic chains of the lipids followed by a sudden increase of their lateral mobility. For this reason, the higher temperature phase is called liquid disordered, whereas that at lower temperature solid ordered. According to this description, the phase state of a lipid bilayer can be described by an order parameter related to the possible conformations of the hydrocarbon chains. The transition temperature is strongly related to the length of the acyl chains of the lipids and to the possible presence of one or more double bonds in the chains[26-28]. However, also the headgroups of lipid molecules have an effect on the lipid phase transition temperature[29]. This is due to electrostatic dipolar interactions. Phospholipids with the same hydrophobic chains but with different headgroups can have transition temperature separated by more than 20°C. The transition from the solid ordered to the liquid disordered phase implies an increase (up to 25%) of the lateral area per lipid, due to the increased disorder of the hydrophobic chains. From this, an increased lateral mobility derives. At the same time, the thickness of the lipid bilayer decreases so that, globally, the volume increases only by 3-4%. Therefore, the transition could be approximated by a constant volume phase transition. This is true for bilayers which can accommodate for the increased lateral area without increasing their tension. The main phase transition is considered, after a long debate, mainly a first order phase transition in which several properties of the bilayer change suddenly as the transition temperature is crossed[30]. However, even if the transition is considered first order, a lipid bilayer composed by only one type of lipids can show extended phase coexistence regions. This is mainly due to a reduced cooperativity and to the presence of both short- and long-range interactions between the lipids in the bilayer. Some lipids, in particular conditions, can produce a ripple phase in the bilayer during transition from the ordered phase to the liquid disordered one. This phase is characterized by a periodic bilayer undulation.

The main experimental technique to study the thermodynamics of the main phase transition is represented by Differential Scanning Calorimetry (DSC)[31]. This technique provides a measurement of the excess heat capacity of lipid dispersions as a function of temperature. Moreover, in the case of mixtures, it is possible to study the mixing behavior of the lipids as a function of the relative fraction of the two components defining a phase diagram.

Another relevant phase transition in these systems is related to the presence of cholesterol[32]. Cholesterol stabilizes the membranes by ordering the lipid acyl chains . This effect is the result of the rigid planar structure of cholesterol. At the same time, if cholesterol partitions in solid domains of a lipid bilayer, it tends to disorder the bilayer structure. This particular effect of cholesterol on a lipid bilayer has been translated in the creation of a new phase in a lipid bilayer which has been named liquid ordered phase. The name refers to both the ordered structure of the hydrophobic chains and to the preserved high lateral diffusion in these domains. Due to the presence of this new phase, the previously defined gel phase has been renamed to solid ordered phase and the liquid crystalline phase has been renamed to liquid disordered phase. However, the presence of cholesterol in lipid bilayers introduces a great complexity in the phase behavior of these structures. Studies on model systems presented some behaviors that were not found in biological membranes; as a consequence, until the introduction of the lipid raft hypothesis in biological membranes[33], the biological community was not particularly interested in this new phase. Later on, the presence of detergent insoluble domains, named lipid rafts, in biological membranes was associated with that of cholesterol and the insoluble domains were connected to the liquid ordered phase previously found in model systems. The definition of lipid rafts has evolved since their first introduction and these are now considered small (about 20-50 nm) domains enriched in cholesterol and sphyngomielin with a dynamical structure in the time scale of ms[34-35]. The introduction of the liquid ordered phase brought about concepts related to fluctuations and critical phenomena in the field of membrane biophysics[36]. Experiments on model systems focused on ternary lipid mixtures which included a high melting temperature lipid, a low melting temperature one and cholesterol. The phase diagram for these mixtures might foresee the presence of a coexistence region of liquid ordered and liquid disordered phases separated from homogeneous phases. The transition from the immiscibility region to the homogeneous one might occur through a critical point. Around this point the two phases are almost indistinguishable and for temperatures above the critical region fluctuations play a dominant role. According to some interpretations, the lipid rafts might be identified with fluctuations in lipid compositions resulting in domains with a small correlation length[8].

3. Preparation techniques and chemical-physical properties of Supported Lipid Bilayers

Supported Lipid Bilayers (SLBs) are assembled on a rigid, typically hydrophilic, substrate such as glass, silicon (di)oxide or mica (Figure 2). Even if specific properties of supported bilayers might depend on substrate nature, we will start with a general introduction to these model systems and we will come back later to aspects related to the type of substrate used. SLBs were initially developed by the McConnell's group to study the interaction of cells with lipid bilayers[22]. They can be assembled following two different strategies: the Langmuir Blodgett/Schaefer approach[19] and the vesicle fusion technique[37]. The first technique is based on two consecutive transfers onto a solid substrate of a lipid monolayer formed at the liquid/air interface in a Langmuir trough. An appealing feature of this approach is in the possibility of imparting transbilayer compositional asymmetry, reproducing thus the actual situation found in biological

membranes, where a lipid compositional asymmetry is established and maintained by active macromolecular systems (enzymes). Moreover, using the Langmuir Blodgett approach, it is possible to fine-tune the lateral pressure of each leaflet controlling also the physical vertical asymmetry in the bilayer. However, it has been shown that, due to rapid (if compared to measuring time) flip-flop transitions in these systems, especially at phase transitions, it is difficult to preserve the lipid composition of each leaflet that was present at the liquid-air interface[38].

In both preparation strategies, the presence of a thin water layer between the leaflet nearer to the substrate (proximal leaflet) and the substrate itself allows lipid diffusion to a certain extent[39] (Figure 2). This thin water layer allows also to host transmembrane proteins if only a small portion of them protrudes from the bilayer towards the support. The vesicle fusion technique enables the incorporation of transmembrane proteins in the SLB more easily than the Langmuir-Blodgett/Schaefer one. Even if strategies for the incorporation of detergent-solubilized transmembrane proteins in already formed SLBs have been developed[40], the direct fusion of proteoliposomes on surfaces appears as a more practical approach. A typical AFM image of a SLB on mica in the case of a single lipid component (POPE) is shown in Figure 3. Typically, defect free bilayers are preferred, but the presence of small defects in the bilayer could otherwise be useful to measure the height of the bilayer from the solid support and to assure the presence of a bilayer on the substrate.

It has to be stressed that when working with lipid mixtures an undesired asymmetry in lipid composition might result from the vesicle fusion technique. This asymmetry involves lipid composition but also lipid density (the second possibility concerns also single component lipid bilayers). Due to the presence of the substrate, lipid composition in the two leaflets could not be easily predicted on the basis of the composition used for Small Unilamellar Vesicles (SUVs) or Large Unilamellar Vesicles (LUVs) preparation and a preferential partitioning of some lipid species in a specific leaflet could be obtained, due to different transition temperatures and electrostatic interactions of the lipid headgroups with the specific support[41].

Briefly, the mechanism of SLB formation from unilamellar vesicles in solution foresees the adsorption of the vesicles on a substrate, the rupture of the vesicles and formation of a continuous planar lipid bilayer on the support. However simple this process might seem, a clear mechanistic description of the formation course is not available. Nevertheless, the structure of the supported bilayer might be very relevant for the behavior of the membrane, especially regarding its phase transition. So, it is worthwhile discussing this aspect in more details. The rupture process, when an osmotically induced stress is not present, is due to a balance between the attraction of the lipid bilayer by the support and the curvature stress on the sides of the vesicles[42]. A strong attraction induces a high curvature in the bilayer leading eventually to pore formations and rupturing of the bilayer. A formed planar bilayer might then go in contact with a still intact vesicle and induce the rupturing of the other vesicle[43]. If there is enough lipid material in contact with the surface, this process leads to a continuous planar bilayer. The described process produces a bilayer in which the internal leaflet of the liposomes is now facing the bulk water solution (inside-up orientation). In the literature, the process of SLB formation starting from vesicles in solution has

been simulated by Monte Carlo methods[44] and by molecular dynamics[45]. A recent coarse-grained approach using dissipative particle dynamics simulation highlighted some interesting aspects of SLB formation from vesicles[46]. In particular, this study considered the possible effects of the interaction between the substrate and the lipid bilayer on the final configuration of the planar lipid bilayer. The lipid-bilayer/substrate interaction typically includes the van der Waals force, the electrostatic double-layer force and the hydration force. If we compare this case with bilayer/bilayer interactions in multilamellar systems, we exclude the Helfrich undulation force due to the fact that the substrate usually suppresses undulation fluctuations of the bilayer. One of the most relevant results, in view of its effect on phase transition of SLBs, is that the van der Waals interaction produces a vertical asymmetry in the lipid density of the leaflets. The proximal leaflet (the one nearer to the surface) has a higher lipid density with respect to the distal one (that facing the bulk water solution). As a consequence, also the thickness of the leaflets will be different, with the proximal leaflet thicker than the distal one. The above effect is proportional to the attractive interaction between the support and the lipid bilayer. The vertical density asymmetry introduces also an asymmetry in the lipid diffusion constant between the two bilayers which will be described in more details below considering also experimental results. A different density in the SLB leaflets was also established by Faller et al. using coarse-grained simulations[47]. The above discussed structural aspects of a SLB clearly point to a shift of the thermodynamic phase of the proximal leaflet towards a more condensed phase with respect to the distal one. If the asymmetry is too strong and a strong interleaflet coupling mechanism is not at work, the vertical asymmetry can eventually lead to an independent phase behavior of the two lealfets.

Another largely exploited model system is represented by the polymer-supported lipid bilayer[48]. In this case, the lipid bilayer is not directly facing the solid support, rather, it is separated from it by a soft polymer layer (cushion) enabling an increased lipid lateral mobility. At the same time, the increased thickness of the hydrophilic region between the lipid bilayer and the substrate allows the incorporation of transmembrane proteins with large extra-membraneous portions. The enhanced lateral mobility of both lipids and proteins makes this model system very appealing for the investigation of dynamic aspects of membrane organization. However, polymer-supported lipid bilayers do not assure the required flatness and stability for AFM imaging, so, very few AFM studies have been reported on these systems[49,50]. For example, the effective presence of a lipid bilayer on the substrate can be confirmed by force spectroscopy measurements (see the section focused on the mechanical properties of lipid bilayers) but the presence of the polymer layer could be misleading in the interpretation of the results.

We already pointed out that the van der Waals interaction might induce a vertical asymmetry in lipid density of supported lipid bilayers. Moreover, the presence of an electrostatically charged substrate might induce a lipid composition asymmetry in the case of mixtures of lipids having differently charged headgroups[51]. The electrostatic interaction is embodied in the double layer force, which depends both on the surface charge of the two interacting surfaces and the ionic strength of the solution used to form the bilayer. Mica, the typically exploited substrate for studying SLB with Atomic Force Microscopy, has a negative surface charge in water solution whereas the bilayer surface charge depends on the lipid type. The

decaying length of the double layer force is exponentially related to the presence of electrolytes in solution via the Debye screening length, whose magnitude decreases upon increasing the ionic strength of the solution. In this context divalent ions will be much more efficient in screening surface charges than monovalent ions. The sum of the van der Waals and the double layer interactions, the latter described by Poisson-Boltzmann equation, is considered in the context of the DLVO (Derjaguin-Landau-Verwey-Overbeek) theory[52]. Both the surface charge of the substrate and the surface charge of the lipid bilayer depend on environmental conditions such as pH. By solving the nonlinear Poisson-Boltzmann equation in the special configuration of a supported lipid bilayer it has been shown that for monovalent ion concentration below 200 mM a significant voltage drop is present between the two bilayer interfaces (the potential energy difference is higher than the thermal energy)[51]. In general, the effects of the presence of a transmembrane voltage on the thermodynamics of lipid bilayers are not well understood. The presence of a voltage drop could be able to modify the thermodynamic phase of a lipid bilayer as it has already been demonstrated for lipid monolayers[53]. Considering this aspect, it is possible that supported lipid bilayers, especially for low ionic strength of the solution, are exposed to a transmembrane voltage difference that is not present in the case of liposomes in solution.

In general, a substrate exerts its influence on a bilayer with an interaction stronger on the proximal leaflet than on the distal one. This differential interaction, as we previously discussed, could produce asymmetries in the chemical and physical properties of the two leaflets. An asymmetry can influence what is usually referred to as interleaflet coupling. In the context of supported lipid bilayers and phase transitions, the interleaflet coupling is strictly connected to the presence of domains in register between the two leaflets. The interleaflet coupling in lipid bilayers is at present investigated from both experimental and theoretical points of view[54]. The biophysical relevance of this phenomenon stems from its possible role as a signaling mechanism between the two leaflets of a bilayer and, consequently, between the inner and outer regions of a cell. For example, the natural lipid composition asymmetry found in eukaryotic cell membranes between the inner and outer leaflet, arouses the question if a liquid ordered (raft) domain that can form in the outer leaflet is able to induce a similar domain also in the inner one. This question is biologically relevant, because it has been shown that only the lipid composition of the outer leaflets is able to give rise to the liquid ordered phase[55,56]. In general, it has been found that the interleaflet coupling is strongly dependent on lipid composition of the leaflets, with an important difference between synthetic compositions and natural membrane compositions[57]. The dynamic interdigitation of the lipid chains is considered one of the main phenomena behind interleaflet coupling[56]. This interdigitation could be considered as a phenomenon that increases the entropy of the lipid chains and an entropy loss due to a restricted dynamic interdigitation could be the driving force for maintaining a coupling between the two monolayers. In the specific case of a SLB, Merkel et al. found that, by increasing the packing density of the proximal layer with respect to the distal one, exploiting hybrid bilayers in which the two monolayers are assembled progressively, an increase in the diffusion coefficient of the distal layer was observed, likely due to a decreased interdigitation effect[58]. Accordingly, a strong asymmetry in the lipid density between the two leaflets could decrease interleaflet coupling. Recalling that it has been suggested, on the

basis of simulation studies, that the presence of a substrate increases the proximal leaflet lipid density, the overall situation can be rationalized by the following considerations. If, due to the presence of a substrate, the lipid density of the proximal leaflet exceeds that of the distal leaflet, the interdigitation of the facing portions of the alkyl chains will be hindered, inducing a decreased interleaflet coupling. Different strategies might be adopted to restore a similar lipid density in the two leaflets. The first one is that of using a substrate that does not interact strongly with the bilayer. Typically, a substrate with an extremely low roughness will have a smaller average distance from the bilayer and will consequently interact more strongly with the proximal leaflet. In general, rough surfaces could result in SLBs with physical characteristics more similar to unsuspended lipid bilayers, but the roughness could affect the AFM imaging of the bilayer strongly reducing the possibility of identifying different domains (in some cases, using force spectroscopy it could still be possible to identify the presence of the bilayer even if the lateral resolution prevents its imaging). By choosing a substrate with a larger roughness, without preventing the possibility of clearly detecting different phases in the bilayer, it is possible to reduce the substrate/leaflets interaction down to a point where the interleaflet coupling prevails. Alternatively, it is possible to let the bilayer assemble on a substrate at high temperature (above that of phase transition for the bilayer on the substrate), in order to induce a low lipid density also in the proximal leaflet. The latter approach will prevent the increase of lipid density in the proximal leaflet allowing a stronger chain interdigitation and a consequent coupling of the two leaflets.

Another important topic is connected to the lateral diffusion of both lipids and proteins in SLBs. Dealing with lipid diffusion, the problem could be divided in i) the comparison of lipid diffusion between unsupported and supported lipid bilayers and ii) the evaluation of possible differences in the diffusion between the two leaflets. The relevance of lateral diffusion in these systems stems from the many important biological processes that rely on lateral molecular motion[59]. Typically, the diffusion properties of lipid bilayers are measured with optical microscopy techniques involving fluorescence, such as Fluorescence Correlation Spectroscopy (FCS), Fluorescence Recovery After Photobleaching (FRAP) and Single Particle Tracking (SPT)[60,61]. All these techniques could be also employed on biological membranes, enabling a direct comparison with model systems. On the other hand, model membranes could be exploited to fully understand the information that these techniques can provide under well-established conditions. In general, from optical diffusion studies on lipid bilayers, the structure of the membrane could be inferred. Different features of the observed diffusion can be interpreted on the basis of obstacles present in the bilayer. So, a combination of studies in which the results of optical diffusion experiments are compared to the nano-scale structure obtained by AFM could be of high value in this context[62]. It has also to be considered that the diffusion properties of SLBs depend on the chemical and physical properties of the substrate used to support the membrane[63]. Moreover, due to the subtle dependence of the SLBs properties on their preparation and observation conditions, it is very difficult to compare results obtained in different laboratories. Despite all these considerations, some general trends appear in the literature and they will be discussed in what follows.

Concerning the comparison of the diffusion properties of SLBs with those of other lipid bilayer model systems, experimental results have shown that lipid diffusion in free standing

bilayers (GUVs, Giant Unilamellar Vesicles) is more than two times faster than in supported lipid bilayers (the diffusion coefficient is D = 7.8 $\mu m^2 s^{-1}$ for GUVs and D = 3.1 $\mu m^2 s^{-1}$ for SLBs on mica)[64-66]. The difference in the diffusion constant is usually attributed to the interaction of the substrate with the bilayer or to surface sticking of the lipids creating pinning points between the support and the bilayer. In particular, the presence of pinning points refers to the possibility of localized interactions between the lipid bilayer and the support. For example, if pinning points are present, they could induce the appearance of domains always in the same positions of the bilayer if cycles of increasing and decreasing temperature across the phase transition are performed. Instead, dealing with generic interaction we refer to a diffused and continuous contact between the bilayer and the support.

A different and more complicated issue is the possible difference in the diffusion coefficient of the two leaflets composing a bilayer. In the literature, different results can be found. Hetzer et al.[67] found that the outer leaflet displays a diffusion constant that is two times higher than that of the inner leaflet, pointing to an independent behavior of the two leaflets. Recent results reported the same translational diffusion coefficient for both leaflets within a 10% experimental uncertainty[68]. In the latter case a strong coupling between the two leaflets could be the reason for the same lateral mobility. However, many results show that diffusional behavior and interleaflet coupling are strongly related to experimental details and conditions of sample preparation. Therefore, it is not always possible to compare the obtained results, even if on the same phospholipid and substrate system. Harb and Tinland[69] studied the lipid diffusion in the two leaflets of solid supported lipid bilayers for different ionic strength and for different temperatures. They were able to conclude that low ionic strengths favor a decoupling between the leaflets, whereas the leaflets appeared coupled for ionic strength higher than the one produced by a 100 mM NaCl solution. They also found that the use of a support different from mica allows the observation of higher diffusion coefficients for the lipids in the bilayer and the leaflets resulted always coupled. Studying the diffusion coefficient of the SLBs as a function of temperature, Harb and Tinland observed a clear increase of the diffusion coefficients going from the solid ordered phase to the liquid disordered one. Even in this case, they observed that the variation in the diffusion coefficients depended on the ionic strength of the solution and on the type of substrate used. The different dynamical properties of the two leaflets could have effects on the dynamic coarsening of lipid domains eventually formed in one of the two leaflets.

4 - AFM imaging of lipid phase transitions

4.1 Phospholipid bilayers

In this section we will review some AFM investigations on the main phase transition of supported lipid bilayers. We will consider thermotropic as well as isothermal transitions induced by other parameters such as solution pH. The phase transition of SLBs as compared to the transitions of unsupported bilayers shows some typical behaviors which include: 1) a shift of the transition temperatures to higher values; 2) a decreased cooperativity of the transition (identified

by a temperature range for the phase coexistence larger than in the case of unsupported lipid bilayers); 3) depending on the preparation conditions of the SLBs, two independent transitions, attributed to an independent behavior of the two leaflets, or a single transition might be found by changing the temperature. We will concentrate our discussion on these aspects of the main phase transition as observed with AFM.

Phase separation of lipids is the results of different interaction between lipids of different conformations or different types. For a single lipid component, the interaction between the acyl chains of the same type of lipids produces both the order-disorder phase transition and the corresponding phase separation. The presence of different types of lipids makes the phase separation in the lipid bilayer more complex to be described. We will initially consider AFM experiments on single component SLBs and then we will deal with lipid mixtures.

4.1.1 Single lipid component

Considering a single component SLB, Charrier and Thibaudau[70] analyzed the main phase transition of a DMPC bilayer. Figure 4 shows the sequence of images they obtained heating the sample from 26°C up to 43.6°C. The images exemplify the ability of AFM to easily trace phase transitions in lipid bilayers when the evolution of a new phase introduces domains with a different height with respect to the pre-existing one. AFM can easily detect height variations as low as 0.1 nm. At the beginning of the sequence, at a temperature of 26°C, the lipid bilayer phase is uniform and likely in the solid ordered phase. Increasing temperature, areas with a lower height emerge. These areas represent domains of the liquid disordered phase. Going on increasing temperature, a new homogeneous phase is obtained, likely corresponding to the liquid disordered one. However, if temperature is increased further, a second transition takes place with a behavior quite similar to the first transition. The explanation of the above results has been identified in the independent behavior of the two leaflets due to a small interleaflet coupling in the bilayer. Moreover, Charrier and Thibaudau derived the presence of two transitions at different temperatures from the different lipid density in the leaflet resulting from the preparation procedure of the SLB. Their main point is related to the fact that phase transitions of lipid bilayers on a substrate with which they interact strongly occurs at almost constant surface area and, consequently, at variable lateral pressure. The variation of the transition temperature with lateral pressure can be quantified by using a two dimensional Clausius-Clapeyron equation:

$$\frac{dT_m}{d\Pi} = T_m \frac{\Delta A_0}{\Delta H_0} \qquad [1]$$

where T_m is the phase transition temperature, Π the lateral pressure, ΔA_0 is the change in the lipid molecular area upon phase transition and ΔH_0 is the change of enthalpy associated with the melting transition. From this equation it is possible to derive the fraction of lipids in the fluid phase as a function of temperature, considering the molecular area for the lipids in the two phases. The

theory predicts a quite large range for the phase transition and two separated phase transitions if the lipid density in the two leaflets is considerably different. According to this interpretation, what appears as a low cooperative transition is indeed due to a phase transition occurring at constant area rather than pressure. A recent theoretical investigation confirmed that the phase transition decoupling in lipid bilayer might be related to a nonuniform stress profile ascribable to a different lipid density in the two leaflets[71]. In fact, a similar leaflet decoupling might be observed also in small unilamellar vesicles where the asymmetry between the two leaflets is strong due to the high curvature.

Similar results have been obtained by Mouritsen et al.[72]. They obtained two separate phase transitions and ascribed the transition at lower temperature to the distal leaflet while the higher temperature one to the proximal leaflet. Moreover, the temperature for the distal leaflet transition was found very similar to the one reported for liposomes of the same lipid composition. Accordingly, they concluded that the distal leaflet behavior is very little affected by the presence of the solid support.

On the other hand, always considering solid supported lipid bilayers with single lipid composition, Tokumasu et al.[73] studied the behavior of a DMPC membrane as a function of temperature. By raising temperature they identified small nanometer domains appearing and slowly increasing with temperature. They reported the presence of only one transition for the bilayer which should be interpreted as due to a bilayer with coupled leaflets. By plotting the area fraction of the liquid phase as a function of temperature, they calculated the cooperative unit size for the transition and found a value almost one order of magnitude lower with respect to that found in unsupported lipid bilayers. The cooperative unit refers to the size (in terms of number of molecules) of the smallest independent subsystem during the phase transition. The authors concluded that the large range for the transition in the supported lipid bilayer was due to a low cooperativity of the transition. Moreover, they found that the melting transition occurred at a higher temperature with respect to unsupported lipid bilayers. The exploitation of van't Hoff analysis for lipid phase transitions observed with AFM can be questioned if the real situation is that of a transition occurring at variable tension in the bilayer. However, considering a description based on the Zimm-Bragg model for the solid to liquid transition in supported lipid bilayer, it is possible to derive the cooperative unit by analyzing the liquid fraction as a function of temperature[74]. The cooperativity of the transition is strictly related to the line tension of the forming domains. The stronger the line tension the bigger are the domains which are formed and the higher is the cooperativity. It is possible to relate the first derivative of the function describing the fraction of liquid lipids with respect to temperature to the cooperative unit. In particular, the cooperative unit enthalpy is related to the slope of the curve for a liquid fraction corresponding to 0.5, which is usually chosen to define the transition temperature. Considering then a pseudo-unimolecular reaction characterized by a specific equilibrium constant, the relationship between the van't Hoff enthalpy and the thermodynamic enthalpy can be derived and used to obtain the number of molecules involved in each cooperative unit. A similar approach has been exploited by Szmodis et al. but considering images obtained by imaging ellipsometry[75]. However, this approach should be rigorously considered for lipid bilayers with only one component. Based on these

studies, in which the solid support for the bilayer is mainly represented by mica, it can be concluded that the presence of the support alters the thermodynamics of the lipid bilayer phase transition. In a review by Giocondi et al.[76], a table summarizing results on DMPC and DPPC in the case of liposomes and SLB configurations is reported. The table analyzes the transition temperatures obtained in both situations. It emerges that transition temperatures for SLBs on mica are typically shifted to higher values and the width of the transition is wider with respect to liposomes. Moreover, it is evident that the shift of the transition temperature depends on the type of substrate used. For example, using silicon oxide as a solid support, the main phase transition measured by AFM is very similar to the one reported by DSC[77].

AFM has also been used to image the ripple phase in SLBs. In particular, Mou et al.[78] showed that it is possible to reversibly induce and erase the ripple phase in a single supported bilayer by using a specific buffer at room temperature (Figure 6). The ripple phase is characterized by periodic stripes forming well-defined angles of 60° and 120°. Later on, the ripple phase has been also studied by AFM in the case of supported double lipid bilayers[79].

4.1.2 Lipid mixtures

Dealing with lipid mixture, several experimental data are present in the literature[80-86]. Seeger et al.[87] exploited a mixture of POPE:POPG (the lipid composition typically used to mimic the composition of *E. coli* inner membrane) to investigate the relationship between the preparation conditions of SLBs and their thermodynamic behavior at the phase transition. The phase transition temperature and mixing behavior of the POPE:POPG lipid mixture has been thoroughly characterized by DSC[88]. In particular, the phase transition temperature for pure POPG is -5°C and for pure POPE it is 24°C. Seeger et al. found that the same lipid composition could provide a situation with two independent phase transitions or with a single one[87]. The first case was obtained when the bilayer was prepared at a temperature lower than the phase transition of the bilayer on the surface. This means that the preparation procedure resulted in a SLB in the solid ordered phase. The second case, a single transition, was obtained when the SLB was prepared at higher temperature. Another required condition to obtain a single transition was that of using an imaging solution characterized by high ionic strength (> 50 mM KCl). Figure 6 shows the sequence of AFM images for decreasing temperature. In Figure 6g the fractional occupancy of the different phases in the supported lipid bilayer is reported. The phase in which only one leaflet has undergone phase transition from the liquid disordered to the solid ordered phase is in this case referred to as “intermediate phase”. Interestingly, the height differences of the domains appearing in both transitions are very similar. Figure 6h shows the evolution of the area of the holes which are present in the bilayer. It is clear that the transition at high temperature involve a very small variation of the area of the holes. The obtained variation is around 5%, a figure clearly lower than the area per lipid variation measured for unsupported bilayers. This evidence suggests that the higher temperature transition occurs mainly at constant area. Considering the transition at lower temperature, the area variation of the holes is now larger (about 20%). This value is

similar to what is obtained in unsupported bilayers. Accordingly, the transition temperature in this case is similar to that of liposomes and the transition appears more cooperative with respect to the previous one. Recent reports highlighted the role of the lateral pressure in phase transitions of supported lipid bilayers. The role of lateral pressure is obviously relevant when a transition involves an expansion of the lipid bilayer. For example, even if not studied by AFM, it has been shown that for monofluorinated phospholipids such as F-DPPC, which, upon the main phase transition goes from a liquid disordered phase to a liquid ordered one characterized by interdigitation between the acyl chains, the phase transition upon an increase of temperature appears frustrated and the full transformation of the bilayer to the solid phase is prevented[89]. In the case of monolayers at the air-water interface, there are several data relating the effect of lateral pressure to phase transitions and the structure of domains. In fact, in a Langmuir trough it is very easy to control the pressure parameter by the moving barriers. Lateral pressure in lipid bilayers is more difficult to control. Apart from the results obtained on supported lipid bilayers, recent experiments, exploiting the Micropipette Aspiration Technique, demonstrated that the lateral tension applied to a lipid bilayer might have a large effect on the phase transition of lipid bilayers[90-92]. This is true for the main phase transition, but also for the miscibility transition in ternary lipid bilayers. In these cases, a lateral pressure is applied in the direction of an increase of the average area per lipid, whereas on the supported lipid bilayers the relevant effect is that coming from the opposite direction. However, the results can be extended to both directions. At the same time, the experimental results have been complemented by theoretical investigations confirming the important role played by lateral tension on lipid bilayer phase transitions[93]. Seeger et al.[87] found that assembling the SLB again on mica, but incubating the surface at high temperature, a phase transition with coupled bilayers showing in register domains is obtained. The preparation temperature appears as a control parameter to tune the lateral pressure vertical asymmetry and to produce a bilayer with coupled leaflet or with specific asymmetries. Accordingly, the behavior of SLBs is reminiscent of the thermal history of the liposomes used to assemble the membrane[86]. The high preparation temperature probably induces a lower lipid density in the proximal leaflet. Accordingly, the density asymmetry will be reduced assuring coupled leaflets. The mechanistic explanation for the reduced proximal lipid density resulting in coupled bilayers is not completely clear. One possible explanation stems from the interdigitation of the final portion of the lipid acyl chains that would be favored in case of a small difference in the lipid density. It is interesting to note that for the two cases, uncoupled and coupled leaflets, the kinetics of domain growth is different. In the first case small domains appear and they quickly reach a stable configuration, at least for the higher temperature phase transition. In the case of coupled leaflets the domains appear more rounded, as a consequence of higher line tension resulting from the higher height difference of the growing domains. In contrast, the time required to reach a stable configuration was greatly increased and this situation prevented the acquisition of a plot of the growing solid fraction for the domains as a function of temperature in terms of a sequence of equilibrium states. It is interesting to consider that, between the two extreme cases of completely coupled leaflets and completely separated phase transitions, intermediate case could be found. In this case, it is possible to see an overlap between the phase transitions which manifests itself in the presence of three different domain height levels (Figure 7).

The presence of the substrate with its interaction with the lipid leaflets is the main peculiarity of Supported Lipid Bilayers. It is clear that different substrates might introduce different effects on the SLB. Various hydrophilic substrates with different roughness can be exploited to assemble SLBs, but here we will concentrate only on another substrate which is endowed with the low roughness required to assure good imaging conditions with AFM and the possibility to distinguish different domains which might protrude less than 1 nm form the surrounding phase. This substrate is represented by silicon dioxide. Silicon dioxide surfaces which have been enriched by hydrophilic OH groups allow the formation of SLBs. Seeger et al.[77] compared the behavior of the same lipid mixture (POPE:POPG 3:1) prepared in the same way on mica and silicon dioxide (Figure 8). They found that SLBs prepared on silicon assured always a configuration with coupled leaflets, independently from the preparation temperature. This is at variance with what happens on mica. Moreover, comparing the phase transition as measured with AFM on silicon dioxide (Figure 8e) and that measured by DSC on liposomes, they found that the transitions where slightly separated in temperature whereas the width was very similar. The results obtained on silicon oxide are probably a consequence of the lower interaction between this surface and the lipid bilayer. The reason for the different effect of mica and silicon oxide is probably related to their different roughness, considering that they have similar surface chemical properties. Moreover, it is to be noted that the surfaces which allow only a very small liquid layer between them and a lipid bilayer are the ones which produce the greater shift in the transition temperatures with respect to unsupported vesicles. This situation points both to a sort of dehydration of the lipid headgroups in the lower leaflet inducing a partial lyotropic phase transition towards a more solid phase and to an increased friction between the proximal leaflet and the substrate.

Lipid phase transitions can be affected by many parameters such as solution pH (this effect is related to the surface charge of the lipid bilayers), solution ionic strength, hydrostatic and lateral pressure and the presence of specific ions or impurities. In many cases, the local values of these parameters might be biologically more relevant than a global temperature variation. For example, local variations of pH might represent a biological situation able to induce local phase transitions in lipid bilayers. In principle, every parameter able to shift the phase transition temperature of a lipid bilayer is also able to completely change the phase state of the bilayer. Seeger et al.[77] demonstrated the possibility of inducing a phase transition in a SLB at constant temperature by continuously changing the pH of the solution. Figure 9a reports the DSC traces of a POPE:POPG 3:1 mixture for two different pH values: 7 and 3. For a constant temperature of 27°C, going from a pH 7 to a pH 3, the bilayer goes from the liquid disordered phase to the solid ordered one. The image sequence from Figure 9b to Figure 9f shows the appearance of solid domains while the pH decreases and successively, the domains disappear when the pH is set back to 7. Interestingly, the first domains which appear seem to involve both leaflets but, as the transition proceeds it seems that a flip-flop mechanism brings some lipids from one leaflet to the other.

Considering lipid mixtures, Domènech et al. studied SLBs composed by POPC and cardiolipin (CL) or POPE and cardiolipin[94]. They observed the presence of phase separation in the case of POPE:CL bilayers at different temperatures and, by exploiting the preferential binding of cytochrome c to

the highest domains they concluded that CL should be preferentially included in the highest domains.

Dealing with bilayer compositional asymmetry, Lin et al.[86], exploiting the DLPC/DSPC mixture together with fluorescence microscopy, studied the evolution of the asymmetry connected to a lipid flip-flop mechanism. They established that the flip-flop mainly occurs at the interface between symmetric and asymmetric DSPC domains (Figure 10). They also found that the amount of gel phase in one leaflet with respect to the other is a main determinant for the presence of in registry domains.

4.2 Lipid bilayers containing sterols and other exogenous molecules

As we already pointed out, the introduction of cholesterol in lipid mixture brings about a great complexity in the corresponding phase diagrams. In fact, cholesterol can have different effects depending on its relative concentration. The typically used technique to study membrane domain formation exploits the fluorescence of lipid probes inserted in Giant Liposomes and this approach has been largely used to study phase separation involving the presence of cholesterol. As already stated, the study of bilayers including cholesterol and two other lipids, one with a low melting temperature and one with a high melting temperature is strongly related to the lipid raft hypothesis. Moreover, we already stressed the fact that in biological membranes, if lipid rafts are present, they have a lateral extension around 20-50 nm and are highly dynamic structures. Accordingly, fluorescence imaging technique might not be endowed with the required lateral resolution to study these domains. Instead, AFM appears as the method of choice if nanometer lateral scale domains have to be identified. The probable non-equilibrium situation that might occur in supported lipid bilayers due to the presence of the substrate could resemble that found in cells where the inner leaflet faces the cortical actin cytoskeleton and the presence of membrane proteins could limit lipid lateral diffusion. In fact, in some cases, it has been found that ternary mixtures which give rise to liquid-liquid separation with micrometer scale domains in GUVs do not provide the same kind of domain separation in supported lipid bilayers of the same lipid composition and this behavior has been explained by a non-equilibrium situation for the bilayers on the solid support[95]. However, smaller scale domain separation, not detectable by fluorescence microscopy, has been observed by AFM[96]. The direct visualization by AFM of what are considered lipid rafts have been obtained by Rinia et al.[97] using mixtures of DOPC/eggSM. They also performed detergent extraction at 4°C demonstrating that, at low temperature, only the thinner domains, the liquid disordered ones, were removed, whereas the higher domains, attributed to the liquid ordered phase, remained. In the context of detergent solubilization of lipid bilayers with coexisting liquid ordered and liquid disordered domains, Garner et al.[98] performed an investigation comparing the effects of different detergents on live cells and supported lipid bilayers. AFM was exploited in the investigation of SLBs whereas confocal microscopy was used for live cells. They found a good correlation between the results provided by AFM and by confocal microscopy. They also established that different detergents had different effects and selectivity for the removal of

the liquid disordered fraction. Moreover, the added detergent had an effect also on the shape of the liquid ordered domains, indicating the insertion of the detergent also in the liquid ordered domains. Similarly, El Kirat and Morandat studied by time-lapse AFM the effect of Triton-X-100 on lipid mixtures of DOPC/SM/chol[99] highlighting the capability of AFM to allow a better understanding on the effect of detergents at the nanoscale resolution level. Other studies investigated the presence of lipid rafts in supported lipid bilayers[100-102] and many of them concentrated also on the interaction of specific proteins or peptides and liquid ordered domains due to their hypothesized role as signaling platforms. The dynamic effects of the addition and removal of cholesterol on the phase state of supported lipid bilayers have been studied by Lawrence et al.[103] and by Giocondi et al.[104]. The first group manipulated the cholesterol concentration by using the cholesterol-sequestering agent methyl-β-cyclodextrin which was able to remove cholesterol from the already deposited bilayers of DOPC/SM/chol. As cholesterol was removed, the SM rich domains were dissolved. It is interesting to note that the same procedure applied on living cells demonstrated that the activity of specific membrane proteins were altered[105]. On the contrary, by adding cholesterol to the supported bilayer the SM-rich regions increased and eventually a bilayer with a homogeneous phase appeared. The second group incubated preformed supported lipid bilayer of DOPC/SM with cholesterol-loaded methyl-β-cyclodextrin and monitored the evolution of the bilayer from what has been considered a solid ordered/liquid disordered phase coexistence to a uniform liquid ordered phase. Many of the interpretations of the acquired AFM images in the just described works are based on the measurement of the height difference between the domains. However, this is a critical point in the study of phase transitions by AFM. In fact, it has to be stressed that the measured height of lipid domains is convoluted with their mechanical properties. In the section on the mechanical properties of lipid bilayers at the phase transition, we will discuss in more details this topic. For example, it is very difficult to distinguish a solid ordered domain from a liquid ordered one. In all the cases, dealing with model lipid membranes, the reliable way would be that of measuring the lateral diffusion properties of the lipids in the two phases. Moreover, it has to be considered that in the presence of liquid-liquid phase separation, it is possible to be in a situation near a critical point where the difference between the composition of the coexisting domains can get very small and even below the vertical resolution of the AFM.

Dealing with ternary lipid mixtures, a recent paper by Connell et al.[106] studied the behavior of supported lipid bilayer composed by the mixture DOPC/SM/chol near critical points. They adapted to the AFM case already exploited techniques to determine the phase diagram, including tie lines, in terms of the three-sided Gibbs triangle. Figure 11 shows some examples of the domains found at different temperatures for different lipid compositions. In the bottom of Figure 8 the representation in terms of the Gibbs triangle for the different lipid compositions is reported. The phase diagram reports also the miscibility line and the line of critical points for different temperatures. In the same work the authors showed that approaching a critical point the height difference between the coexisting liquid ordered and liquid disordered domains tends to zero, as would be expected for domains with very similar lipid compositions. It is important to stress that AFM can detect nanometer domains for which fluorescence techniques do not have enough

lateral resolution and the relative proportion of the different domain areas can be quantitatively measured in AFM images. The relative proportion of the domain occupancy can provide another evidence for criticality while the system approaches the homogeneous phase region. In fact, the region near a critical point should be characterized by an equal proportion of the two different lipid phases. Regarding the imaging of ternary lipid mixture for temperatures above the critical region it is to be considered that the study would benefit a lot from the use of high speed AFM imaging to better monitor the fluctuations in lipid composition. However, it is also to be considered that imaging above the critical temperature could be problematic in the case of supported lipid bilayers due to the fluxes of moving lipids associated with compositional fluctuations. In fact, these fluxes could make AFM imaging unstable.

A recent work by Bhatia et al.[107] analyzed the possibility of freezing the domain structure of GUVs on a solid support. This possibility allowed imaging the supported bilayer both by fluorescence microscopy and by AFM. They established that, in the case of the DOPC/DPPC/chol mixture, the extended solid ordered and liquid disordered domains that were easily imaged by fluoresce microscopy were characterized by a substructure of smaller domains of the opposite phase inside (small islands of the solid ordered phase inside the extended liquid disordered phase and vice-versa). This work strongly highlights the added value of AFM in the study of lipid domains.

A special case dealing with the interaction of supported lipid bilayers with exogenous molecules is represented by ethanol and anesthetics in general. This is mainly due to the interest in studying the effect of these molecules on lipid bilayers and to the fact that some of their effects on membrane proteins could be interpreted as indirect effects mediated by a modification of lipid bilayers properties. For example, it is known that alcohols affect the phase transition temperature of lipid bilayers and can induce the interdigitated phase as demonstrated also by AFM imaging. In particular, Mou et al.[108] demonstrated the formation of the interdigitated phase of DPPC and DSPC supported lipid bilayer exposed to ethanol. They also noted how the formation of the new phase was dependent on the thermal history of the bilayer. Also the interaction of the anesthetic halothane with DPPC and DOPC membranes has been largely studied by the Cramb group[109]. They also studied by means of the force curve approach the modifications induced by the anesthetic on the mechanical properties of the lipid bilayer. In an interesting work, Vanegas et al.[110] demonstrated the possibility to construct the phase diagram for the mixture DPPC/ergosterol/ethanol and they also found the simultaneous presence of three different phases in the same bilayer (Figure 12).

5. Kinetics of domain growth

One of the most important added values in the use of AFM in phase transition studies of lipid bilayers is that of being able to measure the kinetics of domain nucleation and growth with high lateral resolution. In the study of domain nucleation the ideal thing would be that of coupling high spatial resolution with high time resolution. In practice it would be important to have a snap-shot of the bilayer at specific time intervals. However, to increase time resolution it is sometimes

required to decrease the lateral resolution in order to find a good compromise. To perform this kind of studies, a temperature controlled set-up with the possibility to rapidly change the temperature of the imaging cell (~10°C/min) is required in order to image the sample at constant temperature immediately after the cooling or heating step with isothermal nucleation conditions. The first investigation on this topic was performed by Giocondi et al.[111] on DOPC and DPPC supported lipid bilayers. In particular, they observed the Ostwald ripening phenomenon in the domain growth after a cooling step of the bilayer. They observed that small domains, after their initial appearance, disappeared in favor of bigger domains. In a series of works, Longo et al studied the domain nucleation behavior for different lipid mixtures[112-115]. They measured the nucleation rate both in the case of symmetric (regarding the two leaflets) distribution of lipids (DOPC:DSPC) and in that of asymmetrically distributed lipids (DOPC:bovine brain cerebroside). Typically, the rate of domain growth is slower in case of symmetric domains. Unfortunately, much commercial AFMs are not endowed, at the moment, with high enough time resolution to follow the first stages of domain nucleation. Typically, for performing these experiments, the highest allowed scanning speed is used while working in contact mode using the deflection signal, but the resolution is still in the order of seconds. This technique allows a good compromise between lateral and time resolutions. Longo et al. found that the nucleation rate depends on the degree of unsaturation in the lipid acyl chains and on the amount of cholesterol in the bilayer. They were also able to determine the line tension for the growing domains because this physical parameter is the main determinant for nucleation growth. From AFM measurements, they established a quadratic relationship between line tension and the height difference of the growing domains.

6. Mechanical properties of lipid bilayers at the phase transition

In recent years, the interest in the role of lipids for determining the function of membrane proteins is constantly increasing[116]. The nature of the possible effects of the membrane on proteins is mainly based on mechanical properties and the energy required to accommodate conformational transitions of the proteins. The Micropipette Aspiration Technique has allowed obtaining information on different deformation modes of the bilayers, bending and stretching, but the information retrieved are on the mesoscale[117]. AFM allows to probe locally the mechanical properties of a lipid bilayer by exploiting the Force Spectroscopy technique[118-120]. Briefly, the AFM tip is pressed on the supported lipid bilayer and, after an initial elastic interaction related to indentation of the lipid bilayer, at a critical force value, the tip jumps through the bilayer and goes immediately in contact with the underlying support. The force value corresponding to the jump through event is a marker of the bilayer stability and of the strength of the fluctuations in the bilayer[121]. Several reviews can be found in the literature dealing with the force spectroscopy technique for the study of supported lipid bilayers[122-124]. Here we will concentrate only on information that can be obtained in the phase transition region[125].

In thermodynamic systems subjected to fluctuations there is a direct proportionality between fluctuations in energy of the system and its heat capacity. The main phase transition of lipid

bilayers is characterized by the presence of an excess heat capacity and, accordingly, the fluctuations in this region are strongly enhanced. This is true also for the fluctuations in lateral area of the lipids. As a consequence, the jump through force is expected to decrease in the phase transition region. Figure 13 shows the distributions of the jump-through force values obtained on a POPE supported lipid bilayer as a function of temperature[120]. If the most probable force value is reported as a function of temperature, upon decreasing the temperature, after an initial increase of the value, a sudden decrease of the force is observed for temperature values below 25°C. AFM imaging below 25°C shows that the bilayer is in the phase coexistence region and the force curves are always acquired in the still remaining liquid disordered regions. It is interesting to note that, if a map of the jump through force values is reported for a bilayer in the phase transition region, the liquid region is characterized by a decreased force value. The interface region between different domains does not apparently show special features. However, it is possible that the force spectroscopy technique does not have enough spatial resolution to highlight special features in the small interface region. The decreased jump through force curve in the phase transition region could be strictly connected to the higher probability of the bilayer to produce lipid pores and to endow the bilayer with an increased permeability. The deceased jump-through force value points to a lower mechanical stability of the bilayer in the liquid disordered region while the system is in the phase coexistence region. In a recent work, Seeger et al.[126] demonstrated that for a prototypical membrane channel (KcsA) incorporated in a POPE:POPG supported bilayer, upon a phase transition induced by a temperature decrease, the protein preferentially partition in the remaining liquid disordered phase. According to what is typically measured by force spectroscopy, the channels will be surrounded by a mechanically softer bilayer. It is interesting to note that the same authors found, in a work on the activity of single KcsA channels, that, when the lipid bilayer is in the phase transition region, the functional properties of the channel are modified[127,128].

The force spectroscopy technique has been applied also to supported lipid bilayers with coexisting liquid disordered and liquid ordered domains. This is usually associated with lipid mixtures involving cholesterol. A recent study by Sullan et al. concentrated on the mechanical stability of coexistent liquid domains in supported lipid bilayers composed by DOPC/SM/Chol[129]. They measured the mechanical properties of both liquid disordered and liquid ordered domains finding and increased stability for the liquid ordered domains. They also exploited dynamic force spectroscopy experiments[119] to study the activation energy for the formation of pores in the lipid bilayers in the different phases. Redondo-Morata et al.[130], applying the force spectroscopy technique on a lipid mixture containing cholesterol, demonstrated that it is possible to reveal the presence of different domains in a supported lipid bilayer on the base of their different mechanical properties even when the domains have a height difference which is too small to be detected by conventional topographic imaging.

Imaging of different domains with AFM could be affected by the force applied by the AFM tip if the stiffness of the domains is different. This aspect is very critical because, due to the lack of analytical sensitivity of the technique, the different phases are detected on the basis of their different height. In the literature, the two most common imaging techniques have been exploited to image supported lipid bilayer: contact mode and intermittent contact mode. By exploiting the

force curve technique it is possible to identify the initial point of contact of the tip with the surface of the supported bilayer and, if the force curve proceeds to the jump-through event, we have the possibility of using the position of the rigid substrate to align force curves obtained on different lipid domains. Figure 14 shows a similar approach to validate the height differences measured by intermittent contact mode on a lipid bilayer with coexisting liquid ordered and liquid disordered phases. Figure 14a and b show the topographic image obtained by intermittent contact and a line section respectively. Figure 11c shows two force curves, aligned with respect to the substrate, obtained on the two phases. From the two force curves it is clear that the measured height difference is a function of the applied force, but, at the same time, it shows that the value measured in intermittent contact mode corresponds to a value which is little affected by the applied force. One advantage of the intermittent contact mode over the contact one is offered by the phase imaging technique that can be exploited to obtain a high lateral resolution signal to discriminate between domains with different mechanical properties.

7. Conclusions and future perspectives

Atomic Force Microscopy added valuable details to the study of lipid phase transitions. In fact AFM can extend the region of accessible lateral scales provided by fluorescence microscopy techniques and can also complement spectroscopic techniques like NMR. AFM is limited to work on SLBs for which some doubts might be raised referring to their biological relevance due to the vertical asymmetry that can be introduced in the bilayer by the presence of the substrate. However, it is to be considered that by carefully choosing the type of substrate and the preparation strategy for the supported bilayer, the vertical asymmetry can be largely eliminated and the bilayer can present coupled leaflet like in the case of large vesicles. Moreover, the asymmetry in the environment for the two leaflets of the bilayer is a situation that can also be found in biological membranes. Recently, lipid bilayers have been assembled on supports in which holes have been produced and their properties have been studied. At the moment mainly the mechanical properties have been studied by AFM, while the imaging possibilities are hampered by the deformation of the bilayer[131-132], but this approach is worthwhile being further developed. AFM offers also the possibility of a mechanical investigation on the nanometer lateral scale of the lipid domains forming while the bilayer is at the phase transition. In the future we expect that an increasing number of studies will be devoted to phase transitions of supported lipid bilayers with reconstituted membrane proteins[126] to allow detecting the partitioning of the proteins as phase separation occurs in the bilayer. We expect also a development of the analytical capabilities of AFM in order to determine the composition of different domains at a nanometer scale lateral resolution. Moreover, coupling AFM with specific analytical techniques[133-137] could greatly enhance the comprehension of how lipid redistribute upon phase separation in the case of mixtures and the identification of elusive differences between domains which have similar height, such as in the case of solid ordered and liquid ordered domains in ternary lipid mixture. A great

breakthrough is also expected from high speed AFM techniques[138]. These techniques will extend the time resolution now allowed for studying phase transition phenomena and if coupled to temperature control, will allow study the kinetics of those phenomena.

References

1 L. A. Bagatolli, J. H. Ipsen, A. C. Simonsen and O. G. Mouritsen, OG, *Prog. Lipid Res*., 2010, *49*, 378

2 E. Sezgin, H. J. Kaiser, T. Baumgart, P. Schwille, K. Simons and I. Levental, *Nat. Protoc*., 2012, **7**, 1042.

3 D. A. Fletcher and R. D. Mullins, *Nature*, 2010, **463**, 485.

4 B. B. Machta, S. Papanikolaou, J. .P Sethna and S. L. Veatch, *Biophys. J*., 2011, **100**, 1668.

5 A. Yethiraj and J. C. Weisshaar, *Biophys. J*., 2007, **93**, 3113.

6 P. F. Almeida, *Biophys. J*., 2014, **106**, 1841.

7 P. Westh, *Soft Matter*, 2009, **5**, 3249.

8 S. L. Veatch, P. Cicuta, P. Sengupta, A. Honerkamp-Smith, D. Holowka and B. Baird, *ACS Chem. Biol*., 2008, **3**, 287.

9 L. Bagatolli and P. B. Sunil Kumar, *Soft Matter*, 2009, **5**, 3234.

10 D. M. Owen and k. Gaus, *Front. Plant. Sci*., 2013, **4**, 503.

11 C. Kuo and R. M. Hochstrasser, *J. Am. Chem. Soc*., 2011, **133**, 4664.

12 H. McConnell and A Radhakrishnan, *Biophys. J.,* 2008, **95**, L22.

13 A. Seelig and J. Seelig, *Biochemistry*, 1974, **13**, 4839.

14 R. N. Lewis and R. N. McElhaney*, Methods Mol. Biol*. 2007, **400**, 207.

15 R. N. Lewis, D. A. Mannock and R. N. McElhaney, *Methods Mol. Biol*., 2007, **400**, 171.

16 A. Alessandrini and P. Facci, *Meas. Sci. Tech*., 2005, **16**, R65.

17 J. Schneider, Y. F. Dufrêne, W. R. Barger and G. U. Lee, *Biophys. J*., 2000, **79**, 1107.

18 Y. F. Dufrêne, T. Boland, J. W. Schneider, W. R. Barger and G. U. Lee, *Faraday Discuss*., 1998, **111**, 79.

19 Y. F. Dufrêne, W. R. Barger, J. B. D. Freen and G. U. Lee, *Langmuir*, 1997, **13**, 4779.

20 L. Picas, P. E. Milhiet and J. Hernández-Borrell*, Chem. Phys. Lipids*, 2012, **165**, 845.

21 E. I. Goksu, J. M. Vanegas, C. D. Blanchette, W. C. Lin and M. L. Longo, *Biochim. Biophys. Acta*., 2009, **1788**, 254.

22 H. M. McConnell, T. H. Watts, R. M. Weis and A. A. Brian, *Biochim. Biophys. Acta*, 1986, **864**, 95.

23 E. T. Castellana and P. S. Cremer, *Surf. Sci. Rep*., 2006, **61**, 429.

24 M. J. Janiak, D. M. Small and G. G. Shipley, *J. Biol. Chem*., 1979, **254**, 6068.

25 J. F. Nagle, *Ann. Rev. Phys. Chem*., 1980, **31**, 157.

26 D. Marsh, *Biochim. Biophys. Acta*., 1991, **1062**, 1.

27 D. Marsh, *Biophys. J*., 1992, **61**, 1036.

28 G. Cevc, *Biochemistry,* 1991, **30**, 7186.

29 J. F. Nagle, *J. Membr. Biol*., 1976, **27**, 233.

30 C. Huang and S. Li, *Biochim. Biophys. Acta*, 1999, **1422**, 273.

31 S. Mabrey and J. M. Sturtevant, *Proc. Natl. Acad. Sci. USA*., 1976, **73**, 3862.

32 J. H. Ipsen, G. Karlström, O. G. Mouritsen, H. Wennerström and M. J. Zuckermann, *Biochim. Biophys. Acta*, 1987, **905**, 162.

33 K. Simons and E. Ikonen, *Nature*, 1997, **387**, 569.

34 K. Simons and M. J. Gerl, *Nat. Rev. Mol. Cell Biol*., 2010, **11**, 688.

35 D. M. Engelman, *Nature*, 2005, **438**, 578.

36 A. R. Honerkamp-Smith, S. L. Veatch and S. L. Keller, *Biochim. Biophys. Acta*., 2009, **1788**, 53.
37 A. A. Brian and H. M. McConnell, *Proc. Natl. Acad. Sci. U.S.A*., 1984, **81**, 6159.
38 J. M. Crane, V. Kiessling and L. K. Tamm, *Langmuir*, 2005, **21**, 1377.
39 B. W. Koenig, S. Kruger, W. J. Orts, C. F. Majkrzak, N. F. Berk, J. V. Silverton and K. Gawrisch, *Langmuir*, 1996, ***12***, 1343.
40 P. E. Milhiet, F. Gubellini, A. Berquand, P. Dosset, J. L. Rigaud, C. Le Grimellec and D. Lévy, *Biophys. J*., 2006, **91**, 3268.
41 H.P. Wacklin, *Langmuir*, 2011, **27**, 7698.
42 R. Lipowsky and U. Seifert, *Mol. Cryst. Liq. Cryst*., 1991, **202**, 17.
43 J. M. Johnson, T. Ha, S. Chu and S. G. Boxer, *Biophys. J*. 2002, **83**, 3371.
44 K. Dimitrievski, E. Reimhult, B. Kasemo and V. P. Zhdanov, *Colloids Surf. B*, 2004, **39**, 77.
45 H. L. Wu, P. Y. Chen, C. L. Chi, H. K. Tsao and Y. J. Sheng, *Soft Matter*, 2013, **9**, 1919.
46 M. Fuhrmans and M. Muller, *Langmuir*, 2013, **29**, 4335.
47 C. Xing and R. Faller, *J. Phys. Chem. B*, 2008, **112**, 7086.
48 M. Tanaka and E. Sackmann, *Nature*, 2005, **437**, 656.
49 L. J. Jeuken, S. D. Connell, P. J. Henderson, R. B. Gennis, S. D. Evans and R.J. Bushby, *J. Am. Chem. Soc*., 2006, **128**, 1711.
50 M. G. Friedrich, V. U. Kirste, J. Zhu, R. B. Gennis, W. Knoll and R.L. Naumann, *J. Phys. Chem. B*, 2008, **112**, 3193.
51 A. P. Shreve, M. C. Howland, A. R. Sapuri-Butti, T. W. Allen and A.N. Parikh, Langmuir, 2008, 24, 13250.
52 H. -J Butt, M. Jaschke and W. Ducker, *Bioelectrochem. Bioenerg*., 1995, **38**, 191.
53 K. Y. C. Lee and H. M. McConnell, *Biophys. J.*, 1995, **68**, 1740.
54 M. D. Collins, *Biophys. J.*, 2008, 94, L32.
55 T. Y. Wang and J. R. Silvius, *Biophys. J*., 2001, **81**, 2762.
56 M. D. Collins and S. L. Keller, *Proc. Natl. Acad. Sci. U.S.A*., 2008, **105**, 124.
57 V. Kiessling, J. M. Crane and L. K. Tamm, *Biophys. J*., 2006, **91**, 3313.
58 R. Merkel, E. Sackmann and E. Evans, *J. Phys. France*, 1989, **50**, 1535.
59 E. Sackmann, *Science*, 1996, **271**, 43.
60 D. Marguet, P. F. Lenne, H. Rigneault and H.T. He, *EMBO J.*, 2006, **25**, 3446.
61 H. T. He and D. Marguet, *Annu. Rev. Phys. Chem*., 2011, **62**, 417.
62 R. Lipowsky and U. Seifert, *Mol. Cryst. Liq. Cryst*., 1991, **202**, 17.
63 J. M. Johnson, T. Ha, S. Chu and S. G. Boxer, *Biophys. J*., 2002, **83**, 3371.
64 K. Dimitrievski, E. Reimhult, B. Kasemo and V. P. Zhdanov, *Colloids Surf. B*, 2004, **39**, 77.
65 T. Dertinger, I. von der Hocht, A. Benda, M. Hof and J. Enderlein, *Langmuir*, 2006, **22**, 9339.
66 L. Guo, J. Y. Har, J. Sankaran, Y. M. Hong, B. Kannan and T. Wohland, *ChemPhysChem*., 2008, **9**, 721.
67 M. Hetzer, S. Heinz, S. Grage and T. M. Bayerl, *Langmuir*, 1998, **14**, 982.
68 L. Zhang and S. Granick, *J. Chem. Phys*., 2005, **123**, 211104.
69 F. Harb and B. Tinland, *Langmuir*, 2013, **29**, 5540.
70 A. Charrier and F. Thibaudau, *Biophys. J.,* 2005, **89**, 1094.
71 A. Lamberg and T. Taniguchi, *Soft Matter*, 2014, **10**, 257.
72 D. Keller, N. B. Larsen, I. M. Møller and O. G. Mouritsen, *Phys. Rev. Lett.* 2005, **94**, 025701.
73 F. A. Tokumasu, J. Jin, G. W. Feigenson and J. A. Dvorak, *Ultramicroscopy*, 2003, **97**, 217.
74 D. Marsh, A. Watts and P. F. Knowles, *Biochim. Biophys. Acta*., 1977, **465**, 500.
75 A. W. Szmodis, C. D. Blachette, A. A. Levchenko, A. Navrotsky, M. L. Longo, C. A. Orme and A. N. Parikh, *Soft Matter*, 2008, **4**, 1161.

76 M. C. Giocondi, D. Yamamoto, E. Lesniewska, P. E. Milhiet, T. Ando and C. Le Grimellec, *Biochim. Biophys. Acta*, 2000, **1798**, 703.
77 H. M Seeger, A. Di Cerbo, A. Alessandrini and P. Facci, *J. Phys. Chem. B*, 2010, **114**, 8926.
78 J. Mou, J. Yang, C. Huang and Z. Shao, *Biochemistry*, 1994, **33**, 4439.
79 T. Kaasgaard, C. Leidy, J. H. Crowe, O. G. Mouritsen and K. Jørgensen, *Biophys. J*. 2003, **85**, 350.
80 T. V. Ratto and M. L. Longo, *Biophys. J.*, 2002, **83**, 3380.
81 M. C. Giocondi, V. Vie, E. Lesniewska, P. E. Milhiet, M. Zinke-Allmang and C. Le Grimellec, *Langmuir*, 2001, **17**, 3862.
82 O. Domènech, L. Redondo, L. Picas, A. Morros, M. T. Montero and J. Hernández-Borrell, *J. Mol. Recognit*., 2007, **20**, 546.
83 O. Domènech, A. Morros, M. E. Cabañas, M. T. Montero and J. Hernández-Borrell, *Ultramicroscopy*, 2007, **107**, 943.
84 L. Picas, M. T. Montero, A. Morros, M. E. Cabañas, B. Seantier, P. E. Milhiet and J Hernández-Borrell, *J. Phys. Chem. B*., 2009, **113**, 4648.
85 A. R. Burns, *Langmuir*, 2003, **19**, 8358.
86 W. –C. Lin, C. D. Blanchette, T. V. Ratto and M. L. Longo, *Biophys. J*., 2006, **90**, 228.
87 H. M. Seeger, G. Marino, A. Alessandrini and P. Facci, *Biophys. J*., 2009, **97**, 1067.
88 B. Pozo Navas, K. Lohner, G. Deutsch, E. Sevcsik, K. A. Riske, R. Dimova, P. Garidel, and G. Pabst, *Biochim. Biophys. Acta*., 2005, **1716**, 40.
89 B. Sanii, A. W. Szmodis, D. A. Bricarello, A. E. Oliver and A. N. Parikh, *J. Phys. Chem. B*, 2010, **114**, 215.
90 T. Hamada, Y. Kishimoto, T. Nagasaki and M. Takagi, *Soft Matter*, 2011, **7**, 9061.
91 T. Portet, S. E. Gordon and S. L. Keller, *Biophys. J.*, 2012, **103**, L35.
92 D. Chen and M. M. Santore, *Proc. Natl. Acad. Sci. U S A*., 2014, **111**, 179.
93 M. J. Uline, M. Schick and I. Szleifer, *Biophys. J.*, 2012, **102**, 517.
94 O. Domènech, F. Sanz, M. T. Montero and J. Hernández-Borrell, *Biochim. Biophys. Acta*., 2006, **1758**, 213.
95 B. L. Stottrup, S. L. Veatch, S. L. Keller, *Biophys. J*., 2004, **86**, 2942.
96 B. Y. van Duyl, D. Ganchev, V. Chupin, B. de Kruijff, J. A. Killian, *FEBS Lett*., 2003, **547**, 101.
97 H. A. Rinia, M. M. Snel, J. P. van der Eerden and B. de Kruijff, *FEBS Lett*., 2001, **501**, 92.
98 A. E. Garner, D. A. Smith and N. M. Hooper, *Biophys. J*., 2008, **94**, 1326.
99 K. El Kirat and S. Morandat, *Biochim. Biophys. Acta*., 2007, **1768**, 2300.
100 P. E. Milhiet, M. C. Giocondi, O. Baghdadi, F. Ronzon, B. Roux and C. Le Grimellec, *EMBO Rep*., 2002, **3**, 485.
101 D. E. Saslowsky, J. Lawrence, X. Ren, D. A. Brown, R. M. Henderson and J. M. Edwardson, *J. Biol. Chem*., 2002, **277**, 26966.
102 M. C. Giocondi, V. Vié, E. Lesniewska, J. P. Goudonnet and C. Le Grimellec, *J. Struct. Biol*., 2000, **131**, 38.
103 J. C. Lawrence, D. E. Saslowsky, J. M. Edwardson and R. M. Henderson, *Biophys. J*., 2003, **84**, 1827.
104 M. C. Giocondi, P. E. Milhiet, P. Dosset and C. Le Grimellec, *Biophys. J*., 2004, **86**, 861.
105 P. J. Bennett and M. A. Simmonds, *Br. J. Pharmacol*., 1996, **117**, 87.
106 S. D. Connell, G. Heath, P. D. Olmsted and A. Kisil, *Faraday Discuss*., 2013, **161**, 91.
107 T. Bhatia, P. Husen, J. H. Ipsen, L. A. Bagatolli and A. C. Simonsen, *Biochim. Biophys. Acta*., 2014, doi: 10.1016/j.bbamem.2014.05.016.
108 J. Mou, J. Yang, C. Huang and Z. Shao, *Biochemistry*, 1994, **33**, 9981.
109 Z. Leonenko, E. Finot and D. Cramb, *Biochim. Biophys. Acta*, 2006, **1758**, 487.

110 J. M. Vanegas, R. Faller and M. L. Longo, *Langmuir*, 2010, **26**, 10415.
111 M. C. Giocondi, V. Vie, E. Lesniewska, P. E. Milhiet, M. Zinke-Allmang and C. Le Grimellec, *Langmuir*, 2001, **17**, 1653.
112 C. D. Blanchette, W. C. Lin, T. V. Ratto and M. L. Longo, *Biophys. J.*, 2006, **90**, 4466.
113 C. D. Blanchette, W. C. Lin, C. A. Orme, T. V. Ratto and M. L. Longo, *Langmuir*, 2007, **23**, 5875.
114 C. D. Blanchette, W. C. Lin, C. A. Orme, T. V. Ratto and M. L. Longo, *Biophys. J.*, 2008, **94**, 2691.
115 C. D. Blanchette, C. A. Orme, T. V. Ratto and M. L. Longo, *Langmuir*, 2008, **24**, 1219.
116 R. Phillips, T. Ursell, P. Wiggins and P. Sens, *Nature*, 2009, **459**, 379.
117 D. Needham, T. J. McIntosh and E. Evans, *Biochemistry*, 1988, **27**, 4668.
118 Y. F. Dufrêne, T. Boland, J. W. Schneider, W. R. Barger and G. U. Lee, *Faraday Discuss.*, 1998, **111**, 79.
119 A. Alessandrini, H. M. Seeger, T. Caramaschi and P. Facci, *Biophys. J.,* 2012, **103**, 38.
120 A. Alessandrini, H. M. Seeger, A. Di Cerbo, T. Caramaschi and P. Facci, *Soft Matter*, 2011, **7**, 7054.
121 H. J. Butt and V. Franz, *Phys. Rev. E.*, 2002, **66**, 031601.
122 S. Garcia-Manyes and F. Sanz, *Biochim. Biophys. Acta*, 2010, **1798**, 741.
123 A. Alessandrini and P. Facci, *Micron*, 2012, **43**, 1212.
124 J. K. Li, R. M. Sullan and S. Zou, *Langmuir*, 2011, **27**, 1308.
125 S. Garcia-Manyes, G. Oncins and F. Sanz, *Biophys. J.*, 2005, **89**, 4261.
126 H. M. Seeger, C. A. Bortolotti, A. Alessandrini and P. Facci, *J. Phys. Chem. B.*, 2009, **113**, 16654.
127 H. M. Seeger, L. Aldrovandi, A. Alessandrini and P. Facci, *Biophys. J.*, 2010, **99**, 3675.
128 A. Alessandrini and P. Facci, *Commun. Integr. Biol.*, 2011, **4**, 346.
129 R. M. Sullan, J. K. Li, C. Hao, G. C. Walker and S. Zou, *Biophys. J.*, 2010, **99**, 507.
130 L. Redondo-Morata, M. I. Giannotti and F. Sanz, *Langmuir*, 2012, **28**, 12851.
131 S. Steltenkamp, M. M. Müller, M. Deserno, C. Hennesthal, C. Steinem and A. Janshoff, *Biophys. J.*, 2006, **91**, 217.
132 M. Kocun and A. Janshoff, *Small*, 2012, **8**, 847.
133 S. Chiantia, J. Ries, N. Kahya and P. Schwille, *ChemPhysChem.*, 2006, **7**, 2409.
134 J. Oreopoulos and C. M. Yip, *Biophys. J.*, 2009, **96**, 1970.
135 M. L. Kraft, P. K. Weber, M. L. Longo, I. D. Hutcheon and S. G. Boxer, *Science*, 2006, **313**, 1948.
136 L. Opilik, T. Bauer, T. Schmid, J. Stadler and R. Zenobi, *Phys. Chem Chem. Phys.*, 2011, **13**, 9978.
137 J. E. Shaw, R. F. Epand, R. M. Epand, Z. Li, R. Bittman, C. M. Yip, *Biophys. J.*, 2006, **90**, 2170.
138 T. Ando, T. Uchihashi and S. Scheuring, *Chem. Rev.*, 2014, **114**, 3120.

Figure legends

Figure 1: Scheme highlighting the attainable lateral and time scales for different techniques (both microscopic and spectroscopic techniques) exploited to investigate the structure and dynamics of lipid bilayers. The y-axis reports the time scale and it is also endowed with the specification of the different lipid motions with their characteristic time scale. Abbreviations: AFM: Atomic Force Microscopy; NS: Nuclear Scattering; IR: Infra-Red spectroscopy; NMR: Nuclear Magnetic Resonance; SNOM: Near Field Scanning Optical Microscopy; OM: Optical Microscopy; FCS: Fluorescence Correlation Spectroscopy; FRAP: Fluorescence Recovery After Photobleaching; FM: Fluorescence Microscopy.

Figure 2: Schematic representation of the of a supported lipid bilayer. The scheme highlights the presence in the bilayer of a proximal and a distal leaflet according to the distance from the solid support. The scheme underlines also the presence of a thin water layer separating the bilayer from the support.

Figure 3: a) Typical AFM image of a supported lipid bilayer in a homogeneous phase. The presence of small defects and the measurement of their depth (b) allow ascertain the presence of the bilayer on the support.

Figure 4: Sequence of AFM images of a DMPC supported bilayer for different temperatures. It appears that, increasing temperature from 26°C to 43.6°C two phase transitions develop. The higher temperature transition starts when the first transition is already over. The two transitions are ascribed to an independent behavior of the two leaflets. Reprinted with permission from ref 70.

Figure 5: AFM images of a single supported lipid bilayer showing a) boundaries between different ripple domains and b) a spirally grown ripple domain with angles of 60°. Reprinted with permission from ref 78.

Figure 6: a-f) Sequence of AFM images of a POPE:POPG 3:1 supported lipid bilayer at different temperatures: a) 34.5°C; b) 30.4°C; c) 29.1°C; d) 18.6°C; e) 17.3°C; f) 9.5°C. Two independent phase transitions are observed and the evolution of the defects area as the phase transitions proceed is evident. g) Fractional area occupancy as a function of temperature for the liquid fraction (both lipids are in the liquid disordered phase – black squares), the intermediate phase (one liquid is in the liquid disordered phase while the opposite leaflet is in the solid ordered phase – red circles) and the solid phase (both leaflets are in the solid ordered phase – green triangles). h) Area of the defects in the bilayer as a function of temperature. Reprinted with permission from ref. 87.

Figure 7: When a bilayer is assembled on a solid support at intermediate conditions, the independent transitions of the two leaflets overlap and three different levels for the domains appear. The white line is the section relative to the black straight line on the image. Letters S, L and I represent the Solid phase (both leaflets in the solid ordered phase), Liquid phase (both leaflets in the liquid disordered phase) and intermediate phase (the leaflets have different phase), respectively.

Figure 8: (a–d) Sequence of AFM images (image size: 7.5 µm × 7.5 µm) of the same sample area showing the temperature-induced phase transition of a POPE:POPG 3:1 SLB on silicon oxide. Down to a temperature of 22 °C no domain formation was visible. Domains started to appear at 21 °C and extended upon further cooling of the sample. e) The inverse transition enthalpy of Small Unilamellar Vesicles of the same composition, represented by the solid line, is compared to the solid ordered fraction (open circles, the dashed curve is a guide for the eye) of the SLB. The transition on the silicon oxide support occurs at a slightly higher temperature than the one of the SUVs. Reproduced with permission from ref. 77.

Figure 9: (a) Traces of heat capacity of POPE:POPG 3:1 SUVs at pH values of 7 and 3. The curves have been corrected for the effect of the mica support which leads to an increase of the melting temperature by about 5°C. (b) The AFM image (image size: 10 µm x 10 µm, temperature 27°C) at a pH of 7 does not show any lateral heterogeneity. The membrane was prepared at high temperature to ensure a coupling of both leaflets. (c) Starting buffer exchange, at some point (after reaching a pH of about 4) domains started to form. The different height levels in domain 1 indicate that the transition was not fully coupled. (d) Following the evolution of domain 1, it becomes clear that a flip-flop mechanism is present. The initial solid ordered domain changed to an intermediate domain. (e-f) After finally reaching a pH of 3, the buffer was again exchanged for a buffer at pH 7. The intermediate domains vanished demonstrating the reversibility of the transition. Reprinted with permission from ref. 77.

Figure 10: Time-lapse experiment showing the evolution of domains (time unit = 1 h) due to lipid flip-flop. The white dashed arrows point to the symmetric DSPC-asymmetric DSPC interface whereas the white solid arrow point to the symmetric DLPC-symmetric DSPC interface. The black arrow points to a region of fast moving interface characterized by the presence of a fluid DLPC domain. Reprinted with permission from ref 86.

Figure 11: AFM images relative to different compositions for the ternary lipid mixture DOPC/SM/chol. The number or letter in each sequence of images relates to the position on the phase diagram reported below. The sequence of images for different temperatures shows the exit from the phase separation region upon increasing the temperature. The phase diagram below reports the positions of the different lipid mixture, a dashed line representing the phase separation region at 24°C. The dotted line represents the positions of the critical point for increasing temperatures. Reprinted with permission from ref. 106.

Figure 12: In the center, the construction of a phase diagram for the mixture DPPC/ergosterol/ethanol from AFM images is reported. (A–H) Selected tapping-mode AFM images showing domains and phase separation of the phases of interest (Lβ' gel phase, Lβ'I interdigitated gel phase, and Lo Liquid Ordered). All supported lipid bilayers were prepared by vesicle fusion in ethanol/PBS buffer solutions at 65 °C and cooled to 23 °C. Areas labeled with M show defects where the mica support is exposed. Reprinted with permission from ref. 110.

Figure 13: a) Jump-through force distributions on a POPE supported lipid bilayer as a function of temperature. b) Dependence of the jump-through most probable force on the temperature for the

same POPE supported lipid bilayer in a) (the continuous line is a guide to the eye). Reprinted with permission from ref 120.

Figure 14: a) Intermittent contact AFM image of a DOPC/SM/Chol lipid bilayer in the region of liquid disordered and liquid ordered coexistence. B) Line section relative to the dashed white line in a). c) Force curves measured on the liquid disordered domain (red dashed line) and on the liquid ordered domain (black continuous line). The two force curves have been aligned to the position of the underlying substrate. The two straight lines highlight the slope of the contact portion of the two curves. The slopes point out the different stiffness of the two regions.

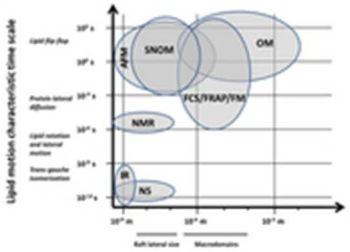

14x11mm (300 x 300 DPI)

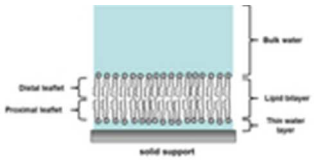

13x6mm (300 x 300 DPI)

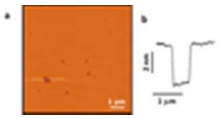

9x4mm (300 x 300 DPI)

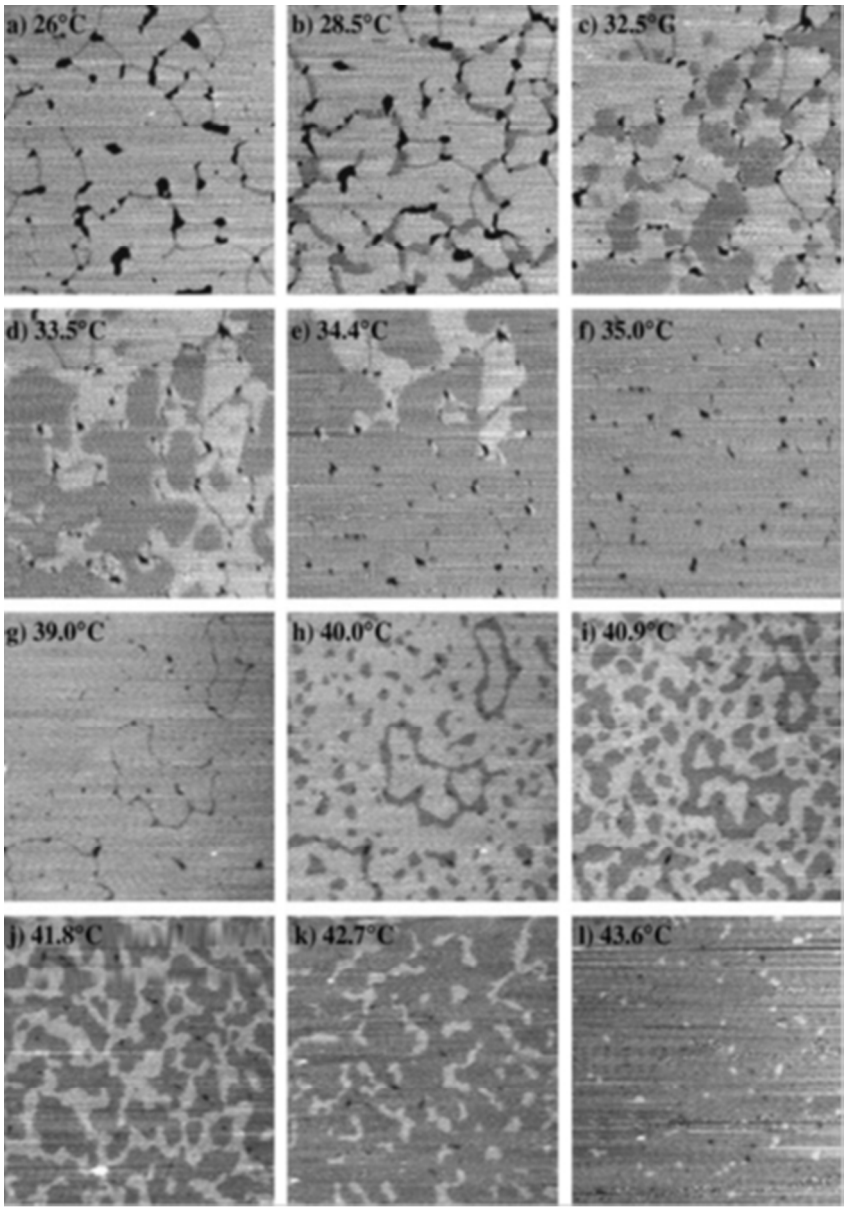

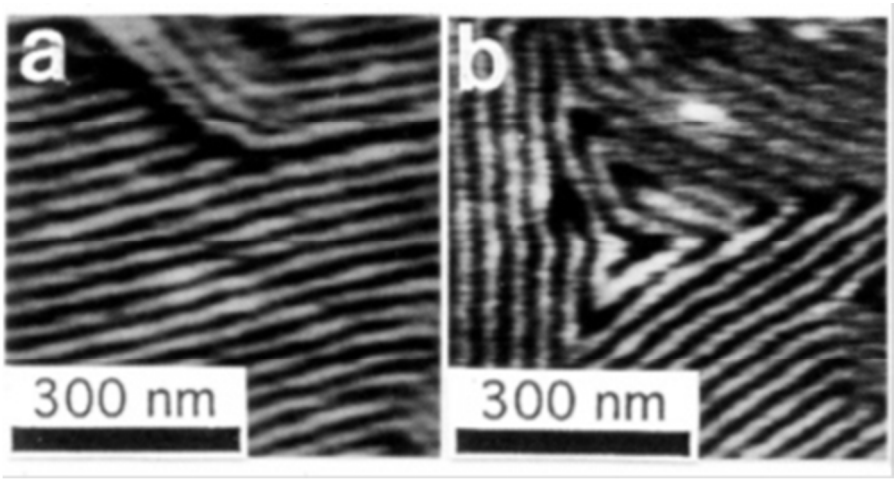

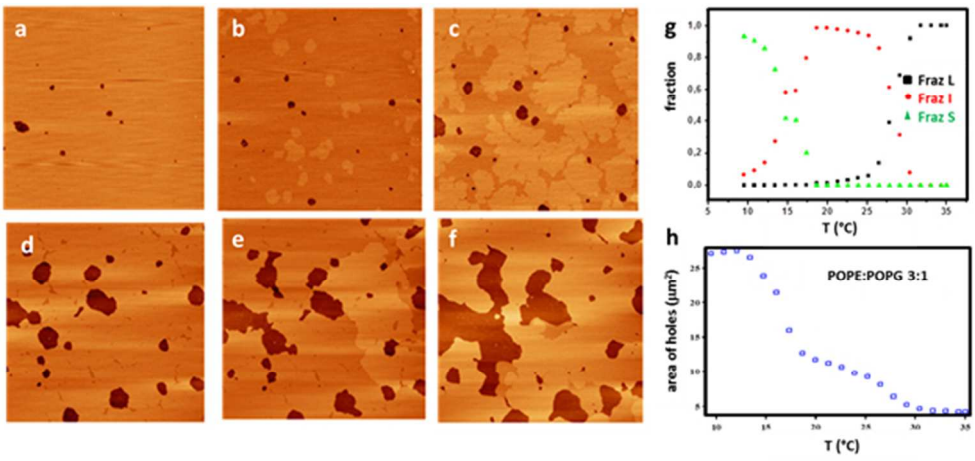

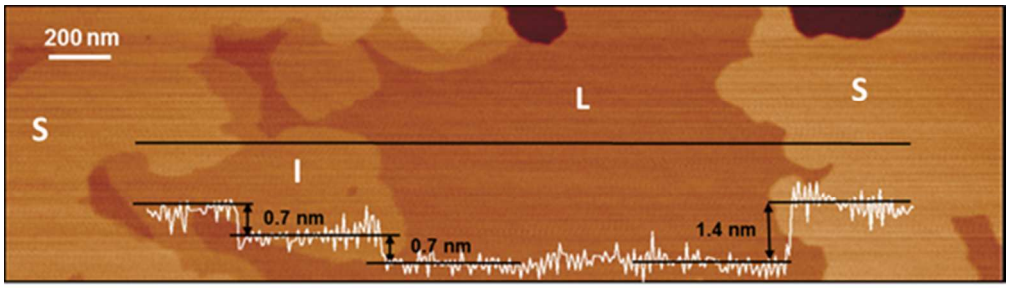

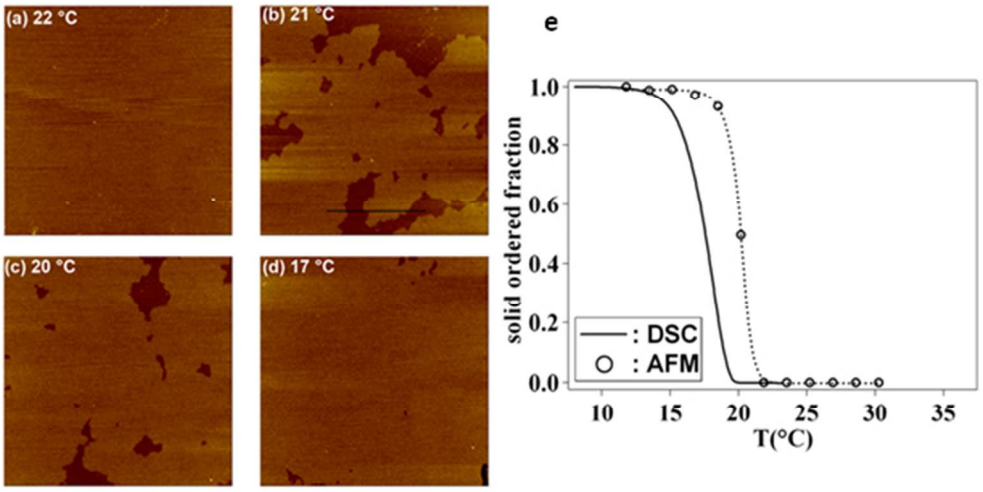

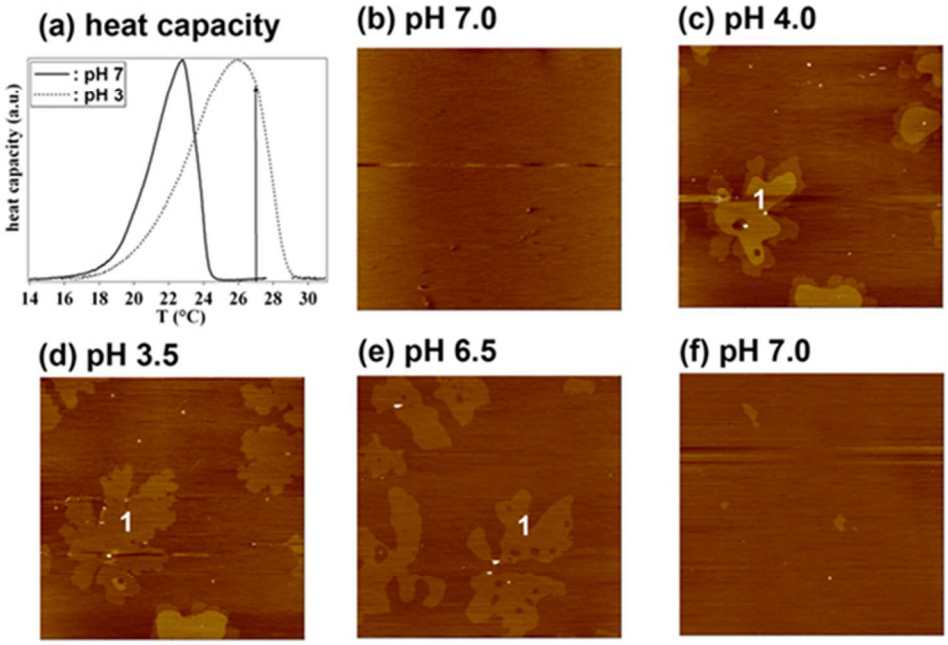

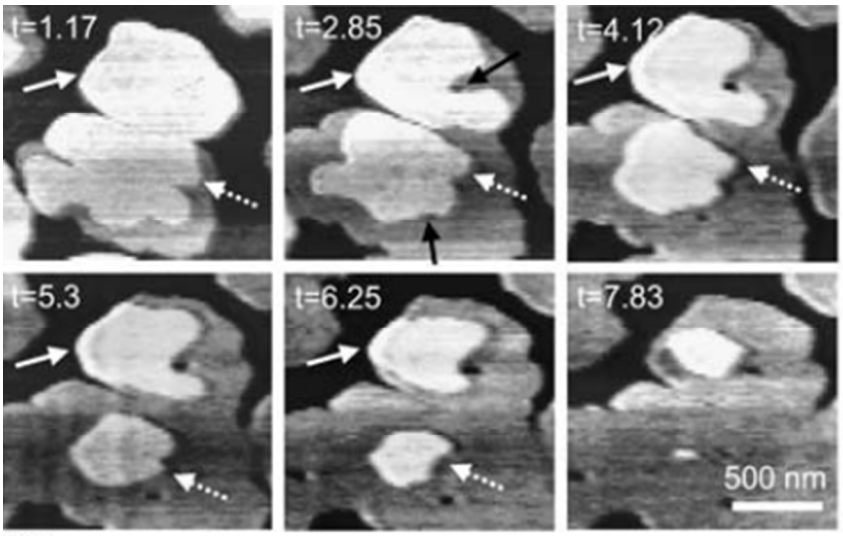

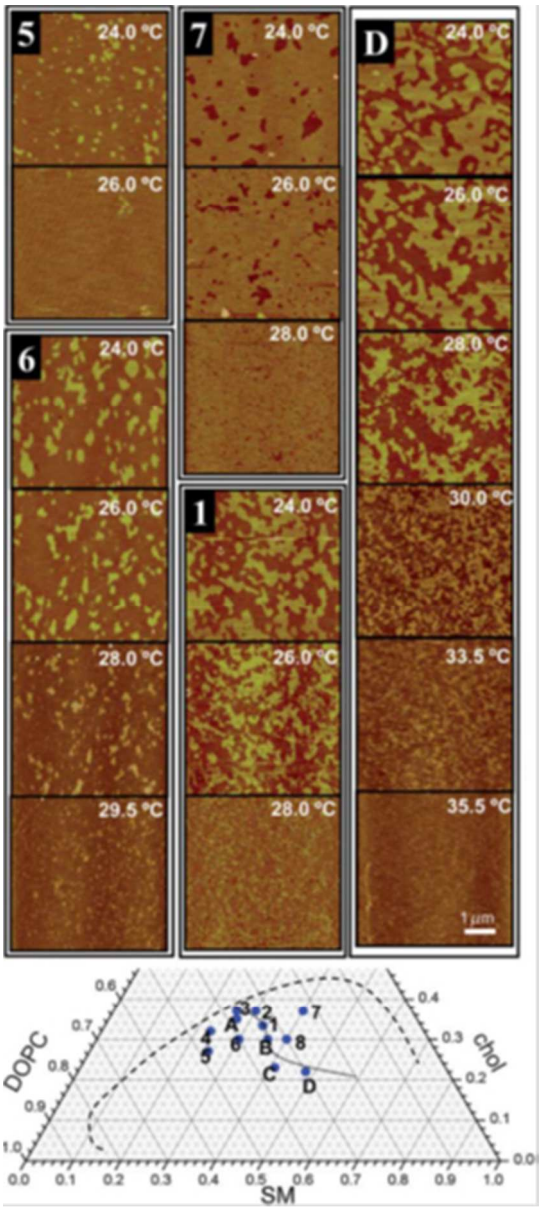

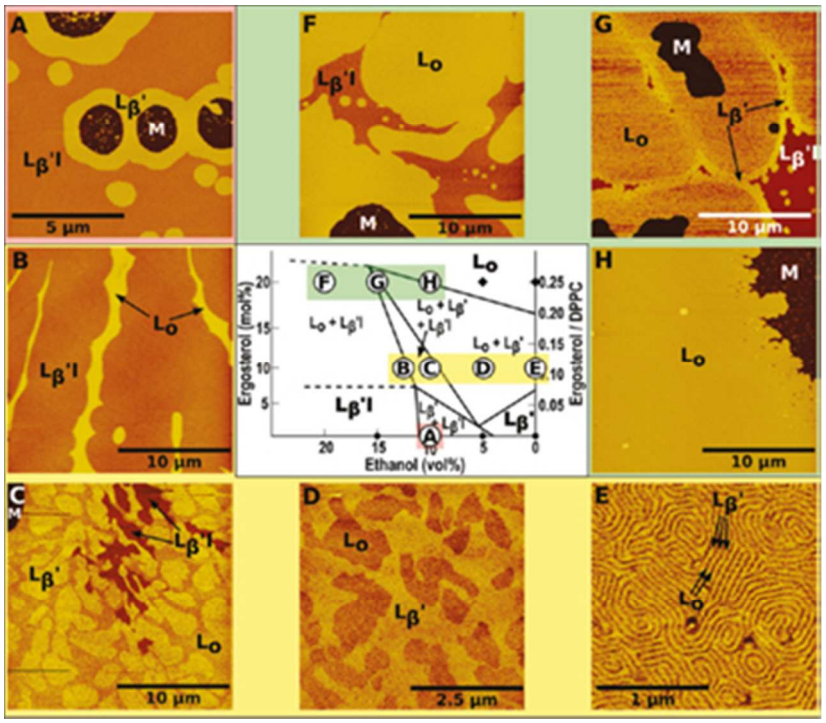

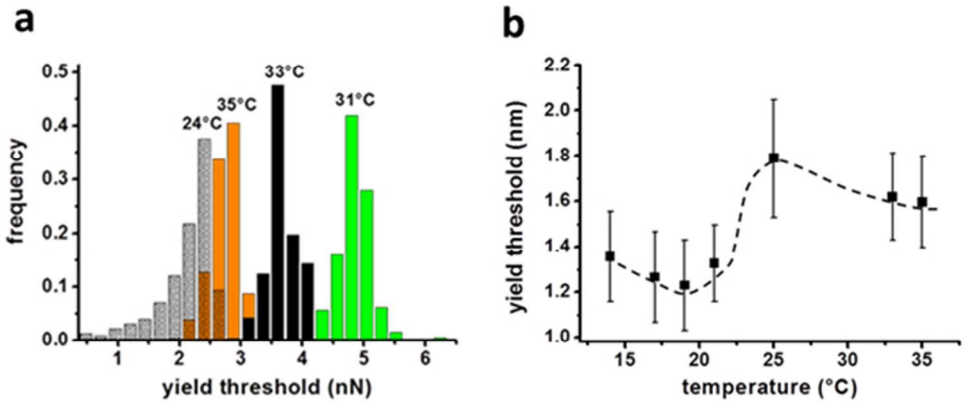

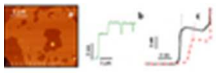

9x3mm (300 x 300 DPI)